ResearchGate

See discussions, stats, and author profiles for this publication at: https://www.researchgate.net/publication/272421454

Local site symmetry of Sm 3 þ in sol–gel derived α 0 –Sr 2 SiO 4 : Probed by emission and fluorescence lifetime spectroscopy

ARTICLE · OCTOBER 2014

READS
26

4 AUTHORS, INCLUDING:

Santosh K. Gupta
Bhabha Atomic Research Centre
58 PUBLICATIONS **603** CITATIONS
SEE PROFILE

Nimai Pathak
Bhabha Atomic Research Centre
16 PUBLICATIONS **25** CITATIONS
SEE PROFILE

Venkatarman Natarajan
Bhabha Atomic Research Centre
159 PUBLICATIONS **1,061** CITATIONS
SEE PROFILE

Available from: Nimai Pathak
Retrieved on: 27 January 2016

Journal of Luminescence ∎ (∎∎∎∎) ∎∎∎–∎∎∎

Contents lists available at ScienceDirect

Journal of Luminescence

journal homepage: www.elsevier.com/locate/jlumin

Local site symmetry of Sm^{3+} in sol–gel derived α′-Sr_2SiO_4: Probed by emission and fluorescence lifetime spectroscopy

Santosh K. Gupta *, N. Pathak, S.K. Thulasidas, V. Natarajan

Radiochemistry Division, Bhabha Atomic Research Centre, Trombay, Mumbai 400085, India

ARTICLE INFO

Article history:
Received 27 August 2014
Received in revised form
1 October 2014
Accepted 6 October 2014

Keywords:
Sm^{3+}
Sr_2SiO_4
Photo-luminescence
Symmetry
Structure

ABSTRACT

Trivalent samarium-doped strontium silicate (Sr_2SiO_4) phosphors were prepared by sol–gel synthesis using tetra ethyl orthosilicate (TEOS) as precursor. The synthesis temperature could be brought down to 600 °C for the formation of a single phase sample. The emission and excitation spectra, and decay curves were employed to study the luminescence properties. The calcined powders of the Sm^{3+} ions doped in the Sr_2SiO_4 emit reddish orange light. In our present study, the $^4G_{5/2} \rightarrow {}^6H_{5/2}$ (MD) transition of Sm^{3+} ions is less intense than $^4G_{5/2} \rightarrow {}^6H_{9/2}$ (ED) transition. This indicates that Sm^{3+} ions preferentially occupy asymmetric site in α-Sr_2SiO_4. Fluorescence life time measurement has shown monoexponential behavior for Sm^{3+} in strontium silicate with lifetime value of 2.23 ms. Based on lifetime and emission spectra, it can be inferred that Sm^{3+} occupies 9-coordinated Sr^{2+} site in strontium silicate. Based on stark splitting pattern it was inferred that site symmetry around Sm^{3+} is C_{3v} which further justifies it's occupancy in 9-coordinated sites. It was observed that, the emission intensity of Sm^{3+} increases with the increase in concentration initially, reaching maxima at 1.0 mol % and then decreases with the increasing concentration due to concentration quenching. At higher concentrations ($x > 0.01$), however, the observed decay curves were bi-exponential.

© 2014 Elsevier B.V. All rights reserved.

1. Introduction

Among the materials currently evaluated as host for lanthanide ions, in this work our attention was focused on alkaline earth silicates. These materials are characterized by good transmission properties in the visible part of the electromagnetic spectrum and by relatively low phonon energies. They can be efficiently doped with lanthanide ions, due to the similarity between the ionic radius of the alkaline earth and the lanthanide ions. Therefore these materials are prospective high efficiency luminophors and are attracting increasing interest for photonics and optoelectronics applications. Indeed alkaline earth silicates are resistant to many chemicals and air exposure and can also be grown with low-cost techniques.

Oxide-based hosts have received considerable attention for use in flat-panel displays due to their luminescent characteristics, stability in high vacuum, and the absence of corrosive gas emission under electron bombardment, as compared to currently used sulfide-based phosphors [1]. Therefore, oxide-based phosphors are likely to emerge as the choice for field emission diodes (FED) green or red phosphors. Among these, strontium silicate is an excellent matrix due to its stable crystal structure, good mechanical strength and high thermal stability provided by the tetrahedral silicate $(SiO_4)^{2-}$ group [2]. Sr_2SiO_4 has attracted interest due to its special structural features and potential application in developing white light-emitting-diodes (LEDs), because GaN (400 nm chip) coated with Sr_2SiO_4: Eu^{2+} exhibits better luminous efficiency than that of industrially available products such as InGaN (460 nm chip) coated with YAG: Ce [3]. The optical band gap of alkaline earth silicate is in the range of 4–7 eV and therefore these materials are characterized by good transmission properties in the visible part of the electromagnetic spectrum.

When an active dopant is introduced into structures with multiple sites (A and B), their optical and magnetic properties are dramatically changed depending on its distribution in the ceramic. Studies of dopant ion distribution among different sites have attracted much attention because they may allow better understanding of the correlations between structure and properties such as color, magnetic behavior, catalytic activity, and optical properties, etc., which are strongly dependent on the occupation of these two sites by metals.

Eu^{3+} is a well known structural probe [2,4–7] because of its non-degenerate ground state $^7F_0$ and non-overlapping $^{2S+1}L_J$ multiplets. Local environment of Eu^{3+} and Dy^{3+} in Sr_2SiO_4 has

* Corresponding author. Tel.: +91 22 25590636; fax: +91 22 25505151.
E-mail address: santufrnd@gmail.co.in (S.K. Gupta).

http://dx.doi.org/10.1016/j.jlumin.2014.10.009
0022-2313/© 2014 Elsevier B.V. All rights reserved.

been reported by our group in our previous work [2,8]. Due to their sharp emission lines; the Sm^{3+} ions could also be used as a luminescent probe [9].

Although reports do exist in the literature on luminescence properties of Sm^{3+} ions in Sr_2SiO_4 [10,11], none of them explain the site occupancy of Sm^{3+} and their related effect on luminescence properties in these matrices. TRES is extensively used to understand such phenomena. In Sr_2SiO_4, there are two types of sites for Sr^{2+}, one is a more symmetric 10 coordinated site Sr (1) and the other is a less symmetric 9 coordinated site Sr (2). We have also tried to investigate the effect of concentration of Sm^{3+} and annealing temperature on its luminescence properties.

2. Experimental results

2.1. Synthesis

All the chemicals used in the sample preparation were of AR grade and procured from Sigma-Aldrich. The alkaline earth silicate samples were prepared via a sol–gel route using tetraethyl orthosilicate (TEOS) and strontium nitrate adopting the standard procedure [12].

2.2. Instrumentation

The phase purity of the prepared phosphors were confirmed by X-ray diffraction (XRD). The measurements were carried out on a STOE X-ray diffractometer equipped with Ni filter, scintillation counter and graphite monochromator. The diffraction patterns were obtained using monochromatic Cu-Kα radiation ($\lambda = 1.5406$ Å) keeping the scan rate at 1 s/step in the scattering angle range (2θ) of 10°–60°. The $K\alpha_2$ reflections were removed by a stripping procedure to obtain accurate lattice constants.

PL data were recorded on an Edinburgh CD-920 unit equipped with a Xe flash lamp as the excitation source. The data acquisition and analysis were done by F-900 software provided by Edinburgh Analytical Instruments, UK.

3. Results and discussion

3.1. Phase purity: X-ray diffraction

Fig. 1 shows the PXRD patterns of undoped and 0.5 mol% Sm^{3+} doped Sr_2SiO_4. The PXRD patterns were in agreement with standard JCPDS no. 39–1256 corresponding to orthorhombic phase. Further no additional peaks can be found in doped samples. Since ionic radius of Sm^{3+} was relatively less when compared to Sr, it was expected that the Sm^{3+} ion can easily enter the Sr lattice without disturbing the crystal structure. It is natural to assume that Sm^{3+} occupies the Sr^{2+} position though cation vacancies are introduced in vicinity to ensure local charge compensation. A structural detail of Sr_2SiO_4 has been given in our previous work [10].

3.2. Photoluminescence excitation and emission spectroscopy

Trivalent samarium ions emit a considerably bright luminescence in the visible and near infrared region in various kinds of host materials. The luminescence bands observed in this ion emission are due to transitions between the energy levels in the $4f^5$ electron configuration. The excitation spectrum of the system at 606 nm emission is shown in Fig. 2. Broad band in the range of 200–275 nm was assigned to the charge transfer band $O^{2-} \rightarrow Sm^{3+}$ (CTB) with λ_{max} at 243 nm. In the wavelength region 320–500 nm, several excitation peaks are observed and are located at 346 nm

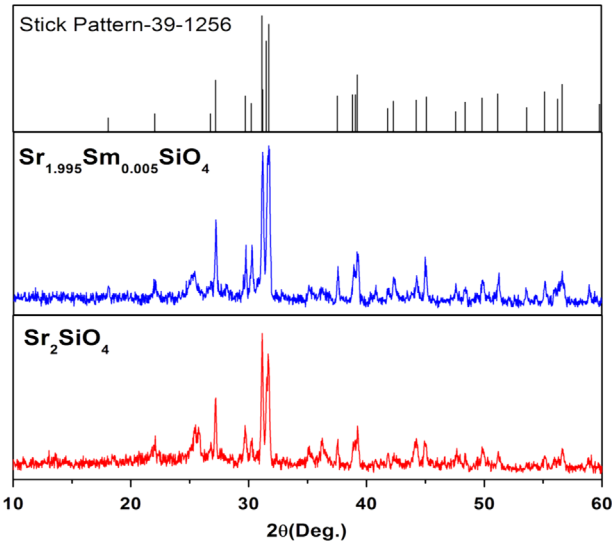

Fig. 1. XRD pattern of the Sr_2SiO_4 and $Sr_{1.995}Sm_{0.005}SiO_4$ powder samples annealed at 600 °C along with standard ICDD stick patterns with file no. 39-1256.

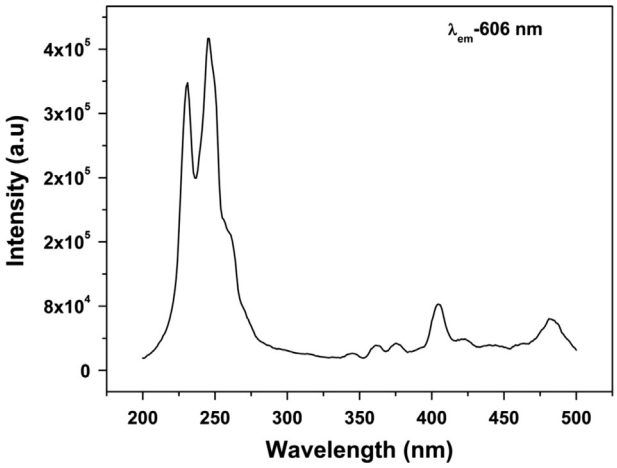

Fig. 2. Room temperature excitation spectra of Sr_2SiO_4:Sm^{3+} (0.5 mol%).

($^6H_{5/2}$–$^6H_{13/2}$), 365 nm ($^6H_{5/2}$–$^4D_{3/2}$), 379 nm ($^6H_{5/2}$–$^6P_{7/2}$), 407 nm ($^6H_{5/2}$–$^4F_{7/2}$), 417 nm ($^6H_{5/2}$–$^6P_{5/2}$), 438 nm ($^6H_{5/2}$–$^4G_{9/2}$), 462 nm ($^6H_{5/2}$–$^4I_{9/2}$), 469 nm ($^6H_{5/2}$–$^4I_{11/2}$), 473 nm ($^6H_{5/2}$–$^4I_{13/2}$) and 485 nm ($^6H_{5/2}$–$^4I_{15/2}$) which are attributed to f–f transitions of Sm^{3+}. From the excitation spectrum, it was found that the intensity of f–f transition at 407 nm is high compared with the other transitions which clearly indicate that these phosphors are effectively excited by near ultraviolet light emitting diodes.

The emission spectra of Sr_2SiO_4:Sm^{3+} phosphor under excitation of 406 nm is shown in Fig. 3. It was observed from the figure that there were four prominent groups of emission lines in the wavelength range of 540–740 nm, which can be attributed to the intra 4f orbital transition from the $^4G_{5/2}$ level to the ^6H_J ($J = 5/2$, 7/2, 9/2 and 11/2). The characteristic emission peaks at 564, 606, 647 and 711 nm for the $^4G_{5/2} \rightarrow {}^6H_{5/2}$, $^4G_{5/2} \rightarrow {}^6H_{7/2}$, $^4G_{5/2} \rightarrow {}^6H_{9/2}$ and $^4G_{5/2} \rightarrow {}^6H_{11/2}$ of Sm^{3+} transitions, respectively. The emission peak at 606 nm ($^4G_{5/2} \rightarrow {}^6H_{7/2}$) was found to be strongest in intensity. The strongest transition $^4G_{5/2} \rightarrow {}^6H_{7/2}$ satisfies the selection rule of $\Delta J = \pm 1$ where J is the angular momentum. Magnetic dipole transition obeys the selection rule of $\Delta J = 0$ and ± 1 and electric dipole transitions only obey the selection rule of $\Delta J' \leq 6$ where J or $J' = 0$ when $\Delta J = 2$, 3, 6 [13]. The peak at 564 nm ($^4G_{5/2} \rightarrow {}^6H_{5/2}$) was a magnetic-dipole transition (MD), the second peak at 606 nm ($^4G_{5/2} \rightarrow {}^6H_{7/2}$) was a partly magnetic and partly a force dielectric-

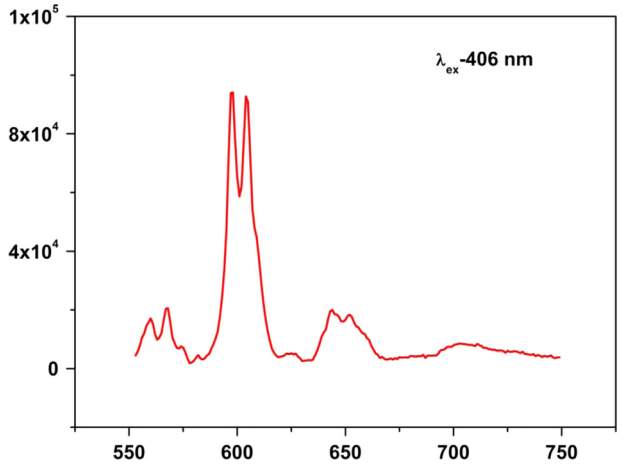

Fig. 3. Room temperature emission spectra of Sr_2SiO_4:Sm^{3+} (0.5 mol%).

dipole transition, and the peak at 647 nm ($^4G_{5/2} \rightarrow {}^6H_{9/2}$) was purely electric dipole transition (ED) which was sensitive to the crystal field [14].

Generally, the intensity ratio of ED and MD (Asymmetry ratio, A_{21}) transitions was used to measure the symmetry of the local environment of the trivalent 4f ions [15] which was sensitive to the nature of the Sm^{3+} ions environment in the host lattice. This gives a measure of the degree of distortion from inversion symmetry of the local environment surrounding the Sm^{3+} ions in the host matrix. Greater the intensity of the ED transition, the more the asymmetry nature. In our present study, the $^4G_{5/2} \rightarrow {}^6H_{9/2}$ (ED) transitions of Sm^{3+} ions were more intense than $^4G_{5/2} \rightarrow {}^6H_{5/2}$ (MD) transition, indicating the asymmetric nature of Sm^{3+} ions in Sr_2SiO_4 host matrix. Consider the ratio between the intensities of the electric dipole transition and magnetic dipole transition. The local symmetry was measured with the relative intensities of these two transitions. The larger value of this ratio means more distortion from the inversion symmetry. The obtained values for A_{21} were found to be 1.18 ($>$ 1), which means that the Sm^{3+} ions were embedded in highly asymmetric environment.

Average ionic radius of Sm^{3+} is around 114 pm, which is closer to 9-coordinated Sr^{2+} (131 pm) and unfavorable geometry in 10-coordination (136 pm) causes most of the Sm^{3+} to occupy 9-coordinated Sr^{2+} sites in strontium silicate. Ionic size and charge differences between Sm^{3+} and Sr^{2+} sites disturbs the local field, where such disturbance is evidenced by the more intense emission of $^4G_{5/2} \rightarrow {}^6H_{9/2}$. It can be concluded that the 9-coordinated strontium polyhedra in host lattice are distorted and there is a lack of inversion symmetry at the Sm^{3+} site.

To get better insight into local site occupancy, PL decay time studies were conducted. The decay curves corresponding to the $^4G_{5/2}$ level of Sm^{3+} ions of 0.5 mol% samarium doped Sr_2SiO_4 is shown in Fig. 4 at excitation wavelength of 406 nm, and with emission wavelength of 606 nm. Fluorescence life time measurement showed monoexponential behavior for Sm^{3+} in strontium silicate with a lifetime value of 2.23 ms. This indicates homogenous environment for Sm^{3+} as can be seen from Fig. 5. Based on lifetime and emission spectra, it can be inferred that Sm^{3+} occupies 9-coordinated Sr^{2+} in strontium silicate.

3.3. Site symmetry around Sm^{3+} in α'-Sr_2SiO_4

When the Sm^{3+} ion is inserted into a chemical environment, the $(2J+1)$-degenerate J-levels are split by ligand-field effects into so-called Stark sub-levels, the number of which depends on the site symmetry of the metal ion. Here again, the Sm^{3+} ion is used as a local crystal-field probe to characterize the structure and site symmetry.

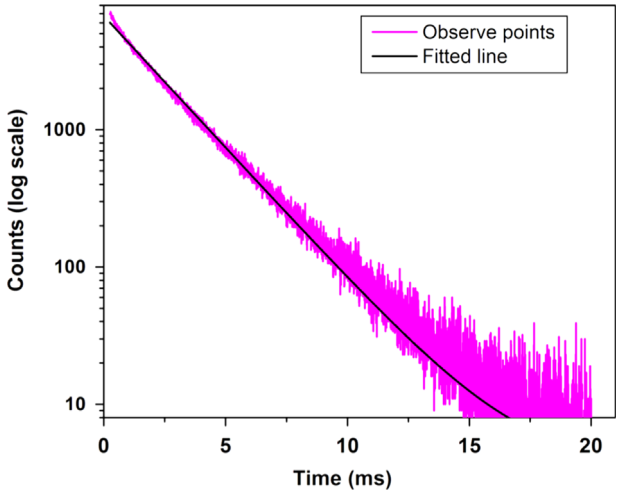

Fig. 4. Room temperature decay curves for the $^4G_{5/2}$ level of Sm^{3+} in Sr_2SiO_4: Sm (0.5 mol%) samples. Samples were excited at 406 nm and emission was monitored at 606 nm.

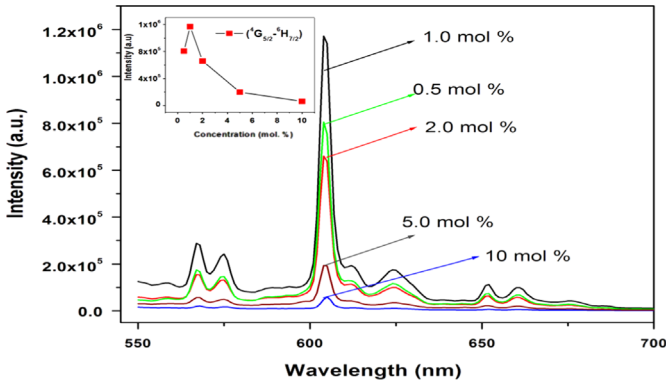

Fig. 5. Variation in PL emission intensity with concentration of dopant ion (λ_{ex}=250 nm). The inset shows relative intensity of the 606 nm emission, normalized to that of the 0.5 mol% doped sample, as a function of the Sm^{3+} content.

The fact that $^4G_{5/2} \rightarrow {}^6H_{9/2}$ line at 647 nm (ED) is very strong in comparison to $^4G_{5/2} \rightarrow {}^6H_{5/2}$ line at 564 nm (MD) indicates that Sm^{3+} occupies asymmetric environment 9-coordinated Sr^{2+} site. From emission and lifetime measurement it is confirmed that site symmetry around Sm^{3+} ion is very low. According to the branching rules of various point groups [16], if for J=2, 3 and 4 number of stark level is 3, 5 and 6 than symmetry will be trigonal and site symmetry will be C_{3v}. As a matter of fact, three lines for J=5/2 $\rightarrow J$=5/2 transition ($\sim$558, 569 and 574 nm), five lines for J=5/2 $\rightarrow J$=7/2 transition ($\sim$582, 598, 604, 610 and 624 nm) and six lines for J=5/2 $\rightarrow J$=9/2 transition ($\sim$639, 643, 646, 652, 656 and 659 nm) of Sm^{3+} were resolved. It infers that the actual site symmetry of Sm^{3+} is very likely reduced to a C_{3v}, due to the difference of ionic radius and charge imbalance between Sm^{3+} and Sr^{2+}. So it can be inferred from these discussions that Sm^{3+} occupies 9-coordinated strontium sites in Sr_2SiO_4 with trigonal symmetry and C_{3v} site symmetry.

3.4. Effect of concentration on emission intensity

To evaluate the emission characteristics of the silicate host with the trivalent samarium ion as dopant, the RE ion concentration was varied from 0.5 mol% to 10 mol%. Fig. 5 shows the dependence

of the PL emission intensity (obtained with $\lambda_{ex}=250$ nm) of the rare earth ion with varying doping concentration.

It was observed that, the emission intensity of Sm^{3+} increases with the increase in concentration initially, reaching maxima at 1.0 mol% and then decreases with the increasing concentration due to concentration quenching. Thus the optimum concentration for Sm^{3+} is 1.0 mol%. The concentration quenching might be due to non-radiative energy transfer from one Sm^{3+} ion to another Sm^{3+} ion. Non-radiative energy transfer takes place via two different mechanisms (i) Forster resonance energy transfer (multipole–multipole interaction) and (ii) Dexter mechanism (exchange interaction).

Forster resonance energy transfer (FRET or FET) is a dynamic quenching mechanism, because energy transfer occurs when the donor is in the excited state. FRET is based on classical dipole–dipole interactions between the transition dipoles of the donor and acceptor and is extremely dependent on the donor–acceptor distance, R, falling off at a rate of $1/R^6$. FRET also depends on the donor–acceptor spectral overlap and the relative orientation of the donor and acceptor transition dipole moments. FRET can typically occur over distances up to 100 Å. Dexter (also known as exchange or coalitional energy transfer) is another dynamic quenching mechanism. Dexter energy transfer is a short-range phenomenon ($\leq$ 10 Å) that decreases with e^{-R} and depends on spatial overlap of donor and quencher molecular orbital's.

In many cases, the concentration quenching is due to energy transfer from one activator to another until an energy sink in the lattice is reached, which is related to the interaction between an activator and another ion. For this reason, it is possible to obtain the critical distance (R_c) from the concentration quenching data. R_c is the critical separation between donor (activator) and acceptor (quenching site), for which the nonradiative transfer rate equals the internal decay rate. Blasse [17] assumed that for the critical concentration the average shortest distance between nearest activator ions is equal to the critical distance.

A rough estimation of the critical transfer distance (R_c) for energy transfer can be obtained using the relation given by Blasse [17].

$$R_C = 2\left(\frac{3V}{4\pi N X_C}\right)^{1/3} \quad (1)$$

where V is the volume of the unit cell, X_C the critical concentration and N is the number of available crystallographic sites occupied by the activator ions in the unit cell. Values of V and N for the crystalline Sr_2SiO_4 (orthorhombic system with primitive lattice, One unit cell of Sr_2SiO_4 comprises of 4 formula units) are 391.2 $Å^3$ and 8, respectively (ICDD card 39-1256). Considering X_C =1% (0.01), critical energy transfer distance R_c in Sr_2SiO_4: Sm^{3+} phosphor was calculated to be 21 Å. In this case, the Sm^{3+}–Sm^{3+} distance is larger than 10 Å. Thus the exchange interactions are ruled out. Therefore, the electric multipolar interaction is believed to be the only mode for the energy transfer among the Sm^{3+} ions in Sr_2SiO_4 phosphor.

Huang [18] and Dai [19] developed a theoretical description on the relationship between luminescent intensity and activator concentration, according to which the mutual interaction type of luminescence quenching in solid phosphors can be concluded by analyzing the constants according to the following equation:

$$\log(I/c) = (-s/d)\log c + \log f \quad (2)$$

where I is the emission intensity, c is the activator content, d is the sample dimension ($d=3$ for energy transfer among the activators inside particles), f is a constant independent of activator concentration, and s is the index of electric multipole. The s values of 6, 8, and 10 are for the dipole–dipole, dipole–quadrupole, and quadrupole–quadrupole electric interactions, respectively, whereas $s=3$ corresponds to exchange interaction.

The $\log(I/c)$ vs $\log(c)$ plot of the 606 nm emission is shown in Fig. 6, from which a slope ($-s/3$) of -2.102 ± 0.288 was derived, yielding an s value of around 6 for the Sm^{3+} doped strontium silicate systems. This indicates that the dipole–dipole interaction may largely be responsible for the observed luminescence quenching of Sm^{3+}.

3.5. Effect of concentration on emission kinetics

The effect of Sm^{3+} content on the $^4G_{5/2} \rightarrow {}^6H_{7/2}$ transition decay curves is shown in Fig. 7 and Table 1. As can be seen from Table 1 monoexponential decay was observed in the diluted samples. At higher concentrations ($x > 0.01$), however, the observed decay curves were bi-exponential, and the bi-exponential changes are more prominent as the concentration of Sm^{3+} increases, revealing that more than one relaxation process exists. When the luminescent centers have different local environments, the associated ions will relax at different rates. If the rates are dramatically different, then diverse decay curves are likely to be observed. Nevertheless, samples with low Sm^{3+} content would minimize the effects of the interactions between optically active ions. Hence, the low-doped samples yield single exponential decay curves with a long lifetime, eliminating this possibility. In addition, it is unlikely that only one site with the shorter lifetime is populated for higher concentrations.

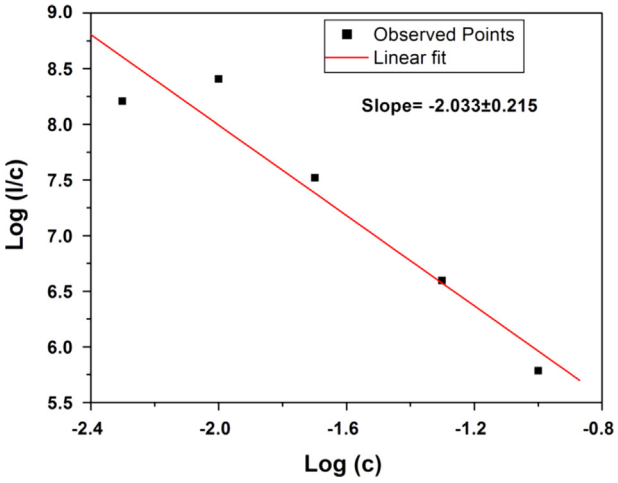

Fig. 6. Relationship between log (I/c) and log(c) for the Sr_2SiO_4:Sm^{3+} phosphor.

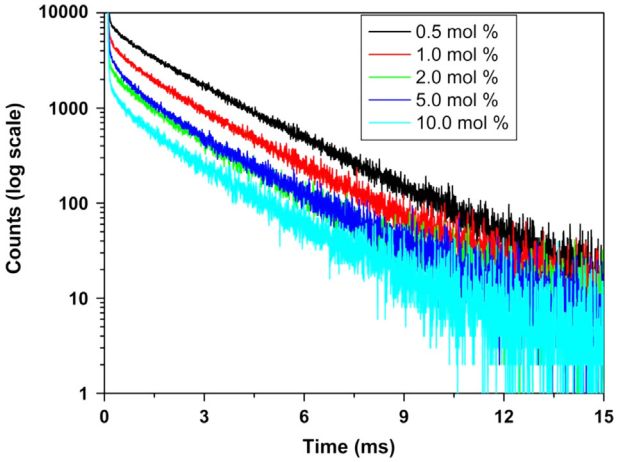

Fig. 7. Decay curves for the $^4G_{5/2}$ level of Sm^{3+} in Sr_2SiO_4: Sm samples for different Sm^{3+} contents. Samples were excited at 406 nm and emission was monitored at 606 nm.

Please cite this article as: S.K. Gupta, et al., J. Lumin. (2014), http://dx.doi.org/10.1016/j.jlumin.2014.10.009

Table 1
Life time values at different dopant concentration.

Mol% of Sm^{3+}	τ_1 (μs)	τ_2 (ms)
0.5	–	2.26
1.0	–	2.33
2.0	569	2.20
5.0	565	2.21
10.0	500	2.13

As mentioned before, cross-relaxation occurs easily between two neighboring rare-earth ions. This is the process whereby excitation energy from an ion decaying from a highly excited state promotes a nearby ion from the ground state to the metastable level. In Sm^{3+}, the energy gap between the $^4G_{5/2}$ and $^6F_{9/2}$ levels is close to that between the $^6H_{5/2}$ and $^6F_{9/2}$ levels. As a result, if the Sm^{3+} concentration is sufficiently high, the higher energy level emission can be easily quenched in favor of the lower energy level emission. Therefore, the energy transfer process between the activator Sm^{3+} ions provides an extra decay channel to change the decay curves, resulting in a non exponential decay curve.

As discussed earlier that there are two crystallographic sites of strontium ion in strontium silicate which can be occupied by Sm^{3+} viz. 9-coordinated Sr (Sr (2)) and 10-coordinated Sr (Sr (1)). Sr (2) polyhedron is much less symmetrical and shares neither edges nor faces with any SiO_4 tetrahedra. Sr (1) polyhedron has more symmetric environment having pseudo-hexagonal symmetry along the *y*-axis. It shares the face and the vertex with the two SiO_4 tetrahedra, which are vertically above and below it and the three edges with three SiO_4 tetrahedra. As can be seen from the Table 1 that at higher concentration ($>x=$ 0.01); two life time values are observed for Sm^{3+} one on the order of 500 μs and the other of the order 2.3 ms. Both these species are present in 9-coordinated environment, but species is having relatively lower life time value is nearer to charge compensating defects and the one having higher lifetime is far off from charge compensating defects.

For Sm^{3+} ions to get incorporated at the Sr^{2+}site three Sr^{2+} ions must be replaced with two Sm^{3+} ions and during this process a cation vacancy is generated in the lattice. This is schematically represented using Kroger–Vink notation as

$$Sr_2SiO_4 \rightarrow V''_{Sr} + 2\left[Sm^{3+}\right]^{\bullet}_{Sr} \quad (3)$$

where V''_{Sr} represents strontium vacancy having two negative charges and $[Sm^{3+}]^{\bullet}_{Sr}$ represent Sm^{3+} occupying Sr^{2+} site with extra positive charge.

A detailed time resolved emission spectrometric study (TRES) was carried out by giving suitable delay times in order to identify the two species responsible for the bi-exponential life times. However, the two emission spectra obtained from the TRES experiments were similar in nature and could not be differentiated.

4. Conclusions

$Sr_2SiO_4:Sm^{3+}$ phosphor were synthesized at 600 °C by the sol–gel route using TEOS as a precursor and characterized by X-ray diffraction (XRD) and photoluminescence (PL) techniques. From the emission spectroscopy the $^4G_{5/2}\rightarrow{}^6H_{9/2}$ (ED) transitions of Sm^{3+} ions were more intense than $^4G_{5/2}\rightarrow{}^6H_{5/2}$ (MD) transition, indicating the asymmetric nature of Sm^{3+} ion in Sr_2SiO_4 host matrix. Fluorescence life time measurement showed monoexponential behavior for Sm^{3+} in strontium silicate with a lifetime value of 2.23 ms. Based on lifetime and emission spectra, it can be inferred that Sm^{3+} occupies 9-coordinated Sr^{2+} in strontium silicate. From crystal field splitting it was inferred that the actual site symmetry of Sm^{3+} is very likely reduced to a C_{3v}, due to the difference of ionic radius and charge imbalance between Sm^{3+} and Sr^{2+}. Concentration quenching of the PL signal intensity was observed for a dopant ion concentration of more than 1 mol%. From this, the critical energy transfer distance of Sm^{3+} was calculated to be 21 Å and the mechanism of concentration quenching was determined to be the dipole–dipole interaction. At higher concentration ($>x=$ 0.01); two life time values are observed for Sm^{3+} one of the order of 500 μs and the other of the order 2.3 ms. Both these species are present in 9-coordinated environment, but species having relatively lower life time value is nearer to charge compensating defects and the one having higher lifetime is far off from charge compensating defects.

Refernces

[1] S.C. Prashantha, B.N. Lakshminarasappa, B.M. Nagabhushana, J. Alloys Compd. 509 (2011) 10185.
[2] S.K. Gupta, M. Mohapatra, S. Kaity, V. Natarajan, S.V. Godbole, J. Lumin. 132 (2012) 1329.
[3] A. Nag, T.R.N. Kutty, J. Mater. Chem. 14 (2004) 1598.
[4] S.K. Gupta, M.K. Bhide, S.V. Godbole, V. Natarajan, J. Am. Ceram. Soc. (2014), http://dx.doi.org/10.1111/jace.13143.
[5] R. Phatak, S.K. Gupta, K. Krishnan, S.K. Sali, S.V. Godbole, A. Das, Dalton Trans. 43 (2014) 3306–3312.
[6] S.K. Gupta, M. Mohapatra, V. Natarajan, S.V. Godbole, RSC Adv. 3 (2013) 20046–20053.
[7] S.K. Gupta, M. Mohapatra, V. Natarajan, S.V. Godbole, J. Mater. Sci. 47 (2012) 3504–3515.
[8] S.K. Gupta, M. Mohapatra, V. Natarajan, S.V. Godbole, Opt. Mater. 35 (2013) 2320.
[9] V. Kiisk, M. Savel, V. Reedo, A. Lukner, I. Sildos, Phys. Procedia 2 (2009) 527.
[10] M.J. Ha, K.R. Han, J.S. Kim, Y.R. Bae, J.P. Kim, J.S. Bae, K.S. Hong, J. Korean Phys. Soc. 64 (2014) 579.
[11] Z. Yang, S. Wang, G. Yang, J. Tian, P. Li, X. Li, J. Chin. Ceram. Soc. 35 (2007) 1587.
[12] T.S. Copeland, B.I. Lee, J. Qi, A.K. Elrod, J. Lumin. 97 (2002) 168.
[13] X.H. Xu, Y.H. Wang, W. Zeng, Y. Gong, J. Electrochem. Soc. 158 (2011) J305–J309.
[14] V.R. Bandi, B.K. Grandhe, M. Jayasimhadri, K. Jang, H.S. Lee, S.S. Yi, J.H. Jeong, J. Cryst. Growth 326 (2011) 120–123.
[15] Santosh K. Gupta, P. Ghosh, N. Pathak, A. Arya, V. Natarajan, RSC Adv. 4 (2014) 29202.
[16] S.V. Eliseevaa, J.C.G. Bunzli, Chem. Soc. Rev. 39 (2010) 189.
[17] G. Blasse, J. Solid State. Chem. 62 (1986) 207.
[18] S. Huang, L. Lou, Chin. J. Lumin. 11 (1990) 36.
[19] Q.L. Dai, H.W. Song, M.Y. Wang, X. Bai, B. Dong, R.F. Qin, X.S. Qu, H. Zhang, J. Phys. Chem. C 112 (2008) 19399.

Please cite this article as: S.K. Gupta, et al., J. Lumin. (2014), http://dx.doi.org/10.1016/j.jlumin.2014.10.009